Far field energy distribution control using a coherent beam combining femtosecond digital laser

Ihsan Fsaifes, Claude-Alban Ranély-Vergé-Dépré, Matthieu Veinhard, Séverine Bellanger, Jean-Christophe Chanteloup

Research Article | Vol. 31, No. 5 / 27 Feb 2023 / Optics Express 8217

Optics EXPRESS

Far field energy distribution control using a coherent beam combining femtosecond digital laser

IHSAN FSAIFES,[1,*] CLAUDE-ALBAN RANÉLY-VERGÉ-DÉPRÉ,[1,2] MATTHIEU VEINHARD,[1] SÉVERINE BELLANGER,[1] AND JEAN-CHRISTOPHE CHANTELOUP[1]

[1]*LULI, CNRS, Ecole Polytechnique, CEA, Sorbonne Université, Institut Polytechnique de Paris–91120 Palaiseau, France*
[2]*Thales LAS France SAS, 2 avenue Gay Lussac, 78995 Elancourt, France*
[*]*ihsan.fsaifes@polytechnique.edu*

Abstract: We report on far field energy distribution control using a coherent beam combining femtosecond digital laser employing 61 tiled channels. Each channel is considered as an individual pixel where amplitude and phase are controlled independently. Applying a phase difference between neighboring fibers or neighboring fiber-lines gives high agility for far field energy distribution and paves the way for deeper exploration of phase patterns as a tool to further improve tiled-aperture CBC laser efficiency and far field shaping on demand.

1. Introduction

Coherent Beam Combining (CBC) of fiber lasers is a promising technique to scale-up peak and average powers of laser systems with beam shaping capabilities. Efforts on CBC developments continue, targeting a wide range of industrial and societal applications [1–5].

CBC relies on the distribution of power to several beams throughout the amplification process before a final coherent addition. In this context, we have built XCAN [5] a CBC femtosecond fiber laser based on 61 tiled channels operating in both high peak and average power regimes. The output beams of 61 independent fiber amplifiers seeded by a common source, are stacked in a hexagonal arrangement and collimated by a high fill factor, 3.2 mm pitch regular hexagonal microlens array. Tiled-aperture CBC allows scaling the number of fibers, but is limited in efficiency since all the energy is not concentrated into the far field main lobe which is indeed surrounded by sidelobes carrying a fraction of energy. The collimating microlens array plays here a major role. As shown by Fig. 1, a fraction of each Gaussian beamlet transverse profile is truncated by its associated individual collimating microlens aperture.

The sidelobes energy is thus determined by the beams array arrangement, which requires a tradeoff between low-filled microlens ($\tau_r < 1$) suffering from sidelobes carrying too much energy in the far-field, and a high-filled aperture ($\tau_r \sim 1$) suffering from clipping energy loss in the near field.

To increase the tiled-aperture CBC efficiency, different methods have been investigated aiming steering the maximum of energy into the main lobe. Beam shaper that transforms the initial Gaussian beam to Super Gaussian or top-hat beams have been used allowing a negligible fraction of truncation losses. A CBC efficiency gain of more than 10% was reported, but specific and complex beam shapers are needed [6–9]. Near field intensity modulation was explored with some improvement on the CBC efficiency [10]. New fiber arrangements like the Bio-inspired sunflower array was proposed; sidelobes weakening and 1% CBC efficiency improvement compared to hexagonal array was reported [11].

#474607 https://doi.org/10.1364/OE.474607
Journal © 2023 Received 1 Sep 2022; revised 24 Dec 2022; accepted 24 Dec 2022; published 21 Feb 2023

Optics EXPRESS

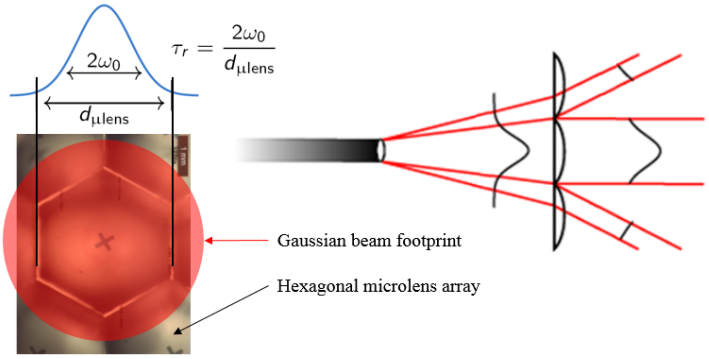

Fig. 1. Illustration of the beam truncation effect by the edge of microlenses. The fill-factor τ_r is defined as the ratio between the beamlets diameter $2\omega_0$ and the short diagonal of the hexagonal microlenses $d_{\mu l}$

The out-of-phase concept in which the phases of the neighboring beams differ by π, was proposed for diffractive coupling of semiconductor lasers by using Talbot effect. This concept allows low edge effect losses, providing a simple means for coherent combining of lasers array [12–14]. Targeting a CBC efficiency improvement through far-field management, A. Andrianov et al. [15] demonstrated a proof-of-concept experiment with CW laser, one-dimensional tiled passive fiber array using out-of-phase pattern where phase differences of π are applied between the neighboring channels. A sound schematic depiction of the concept is displayed in [15] Fig. 1. Considering Gaussian beams, CBC efficiency of 89% is obtained compared to 69% for the "in-phase pattern" in which all beam phases are the same ($\varphi_i = 0$).

In a previous work [16], we have demonstrated that the XCAN laser and its highly scalable architecture can be considered as a digital laser. Tiled aperture offers incontestably high agility in terms of far field beam shaping as each channel is seen as an individual pixel where amplitude and phase are controlled independently. In this paper, we extend the study of out-of-phase concept on our CBC femtosecond digital laser. We explored different phase patterns by applying a phase difference of π between neighboring fibers or neighboring fiber-lines. Improvement of the efficiency achievable with tiled-aperture CBC and field energy distribution are demonstrated. Recommendations for further optimization of tiled CBC architecture are discussed.

2. XCAN in-phase CBC concept

XCAN architecture relies on tiled-aperture configuration, where 61 Yb-fiber amplified laser polarized beams are distributed in the near field side-by-side as close to each other as possible in a planar hexagonal array arrangement (Fig. 2-left). The master oscillator delivers 220 fs laser pulses at a repetition rate of 55 MHz, temporally stretched up to 2.5 ns. For this study, the laser is operated at low power regime, each fiber channel delivering an average power of 2 W. The CBC is achieved when focusing the composite large pupil with a single lens. As illustrated by Fig. 2-right, the electric field transverse distribution observed in this lens focal plane, results from the coherent combining of all 61 beams accurately phased together.

Conventionally, XCAN uses an in-phase pattern (flat phase) in which all 61-beam phases are identical $\varphi_i = 0$. The phase of each individual beam is controlled in real time (kHz) through the combined use of variable optical delay lines and piezo-mechanical fiber stretchers.

The phase stabilization (at ~1 kHz) is performed using an interferometric measurement method with active phase control and a stochastic parallel gradient descent (SPGD) algorithm implemented on a FPGA. The SPGD is used to finely co-phased the 61 beams, allowing a

Optics EXPRESS

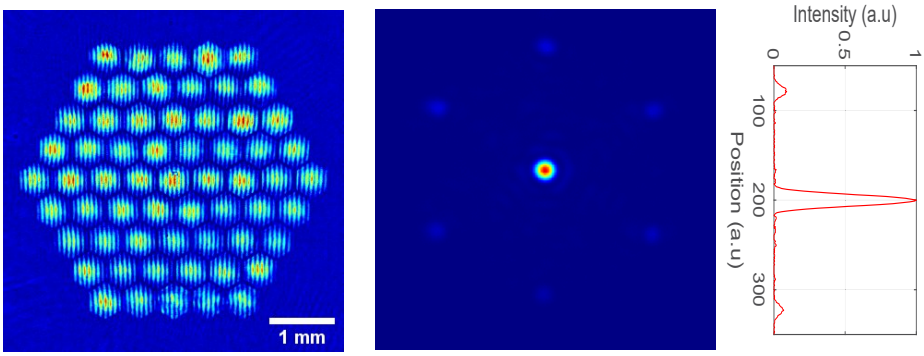

Fig. 2. Left: experimental near field interference pattern of 61 beamlets as operated on XCAN laser. Right: experimental far field obtained after CBC and the corresponding intensity profile.

maximum CBC efficiency to be reached. To maintain a stable CBC efficiency, the XCAN laser incorporates a complete active thermal cooling system. All the amplifiers supporting plates, the laser head and the microlens array mounts are water-cooled.

Fast switchable phase patterns could be generated (in-phase and/or out-of-phase patterns, random. . .) and applied to the CBC laser. Each beam amplitude (i.e., power) could be adjusted through amplifier gain control.

The periodic intensity distribution of the composite beam in the near field gives rise, when a flat phase is applied to all channels, to six similar low-intensities side-lobes surrounding a high intensity main lobe (Fig. 2-right). Thus, the combined beam corresponds only to the main lobe of the far field pattern. The combining efficiency η_{CBC} is defined as the average power in this central lobe divided by the overall average power in the far field. Independently of the number of beams to be combined, the efficiency is limited, theoretically to 67% assuming a perfect laser array and a microlens array fill factor of $\tau_r = 0.93$, experimentally reaching up to 50% with residual phase errors between two fibers lower than $\lambda/90$ RMS. The difference between experimental and theoretical efficiencies is due to misalignments in the fiber array and polarization orientation errors. It's worth noting that all the reported effective combination efficiencies take into account the experimental microlens array transmission (clipping losses) of 92%.

3. Out-of-phase vs. in-phase experimental results

In tiled aperture geometry, a single focusing lens in the beam path is used to perform the optical Fourier transform necessary to obtain the far field. As the composite near field is made of Gaussian output beams, its intensity is periodically modulated, and gives rise, in the far field, to sidelobes surrounding the combined main lobe. The shape of maxima in the far field are determined by the Fourier transform of the beams global envelope in the near field, while the global envelope of the maxima in the far field is determined by the Fourier transform of a single beam. The locations and number of maxima are modified by the phase shifts between the neighboring beams. When all beams are in-phase (flat phase pattern, $\varphi_i = 0$), one maximum beam in the center of the envelope is produced with non-negligible sidelobes. When applying an out-of-phase patterns, i.e. the phase field between neighboring beams differs by π, depending on the fiber array distribution (square, hexagonal,. . .), the maxima in the far field are shifted by half a period relative to the envelope, resulting in the formation of two maxima along each dimension with equal/unequal intensities carrying most of the total power (extra sidelobes are negligible). For example, in case of a square fiber arrangement with 64 fibers and a microlens fill factor of 70%, four equidistant beams are generated with equal intensities (Fig. 3). A second

Optics EXPRESS

CBC stage could thus be possible by using filled aperture technique [15], allowing to improve the CBC efficiency up to 78% instead of 52% in the case of in-phase pattern.

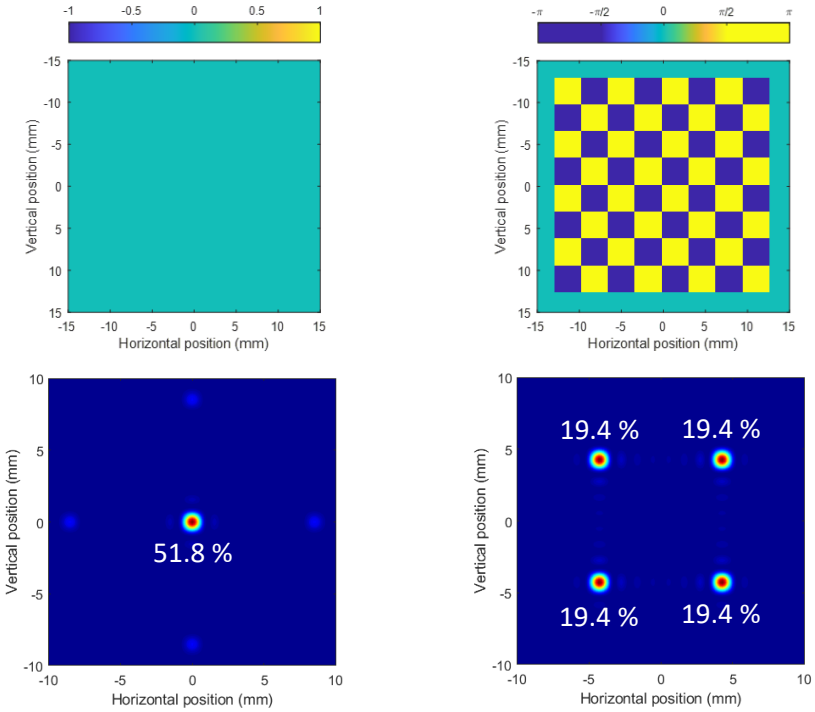

Fig. 3. Left/Right: simulated in-phase/out-of-phase patterns and far fields for 2D square 64 fiber array.

To explore how the field distribution and CBC efficiency evolved, three experimental configurations (1D/2D fiber arrays) are investigated and compared to simulations. For the simulations, an array of Gaussian beams is considered where amplitudes and phases are controlled independently. Each beam gets both collimated and truncated by a dedicated microlens leading to a numerical composite near field. That field is then Fourier transformed in order to model the role of the experimental focusing lens leading then to a numerical far field. Applying the different phase pattern displayed in the following figures allow then to generate the given simulated far fields to be compared with the experimental ones. For all the experimental configurations, the phase correction is performed using an interferometric measurement method with active phase control and beam combination in far field. Thus, the laser is first operated to converge toward a flat phase (in-phase). Then, once the maximum CBC efficiency is achieved through SPGD, the out-of-phase pattern is applied. As we are dealing with a hexagonal beam distribution, a phase difference of π between neighboring fiber-lines instead of neighboring fibers is used.

Configuration 1: this first configuration consists in a fiber-line (1D array) composed of 9 fiber amplifiers (P9), i.e. the middle line of the XCAN hexagonal array with π phase differences between the neighboring fibers. Fig. 4 shows the experimental combined far fields obtained both for in-phase and out-of-phase patterns and compared to simulations. The in-phase pattern leads to a high "on-axis" far-field intensity, while for the out-of-phase pattern a "null on-axis" far field intensity is obtained.

For the in-phase pattern, the measured combining efficiency is 53%, lower than the value obtained by simulation (~70%), due to some discrepancies in the fiber array from a perfect alignment [3].

Optics EXPRESS

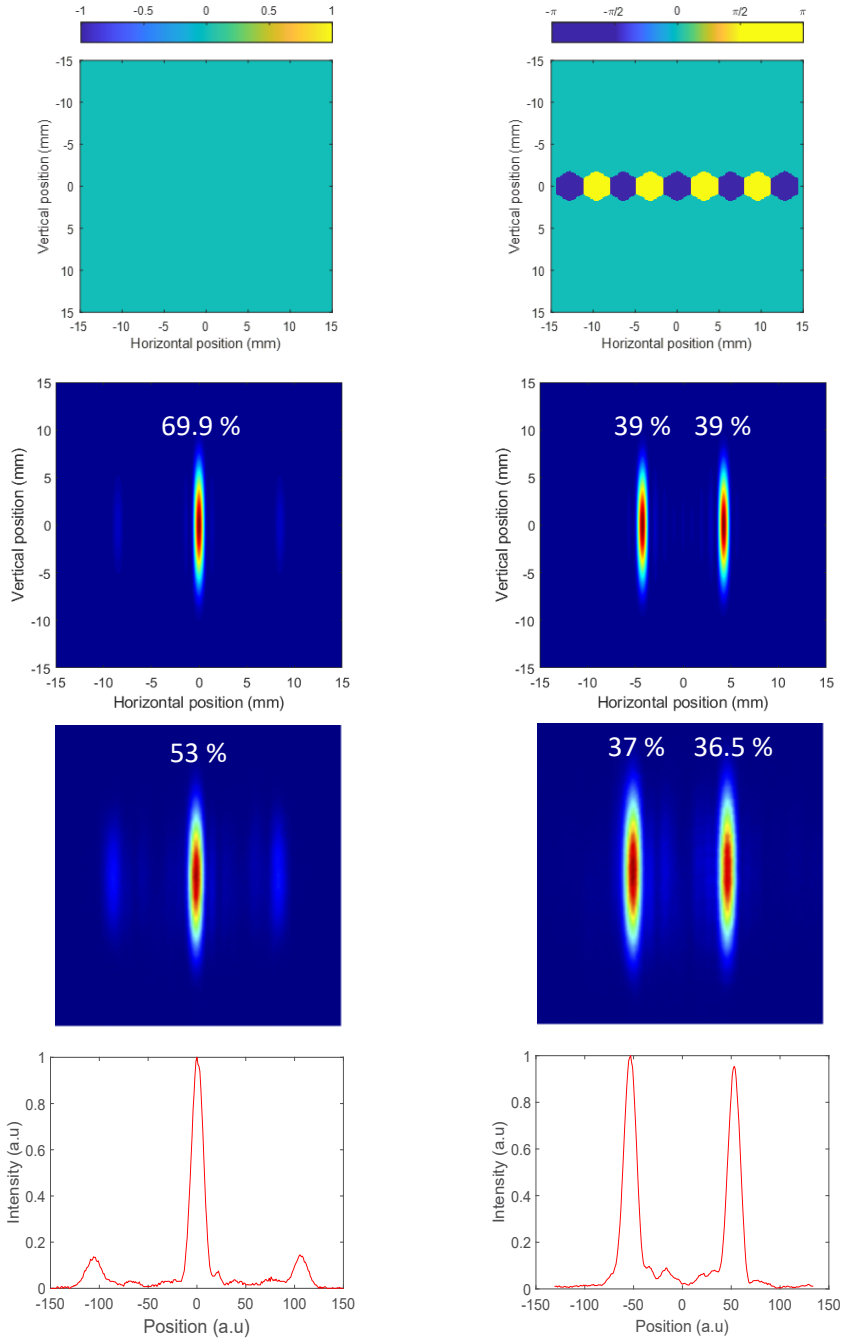

Fig. 4. Left/Right: In-phase/out-of-phase patterns for 1D fiber array (top line), simulated and experimental far fields (2nd and 3rd lines) and experimental intensity profiles (bottom line). Horizontal and vertical scales are identical for simulated and experimental far fields

Two main lobes equally spaced around the center with equal intensities are formed in the far-field with out-of-phase pattern. And, looking at the far field energy distributions, a good agreement is obtained between experimental and simulation results. Experimentally, we observe

Optics EXPRESS

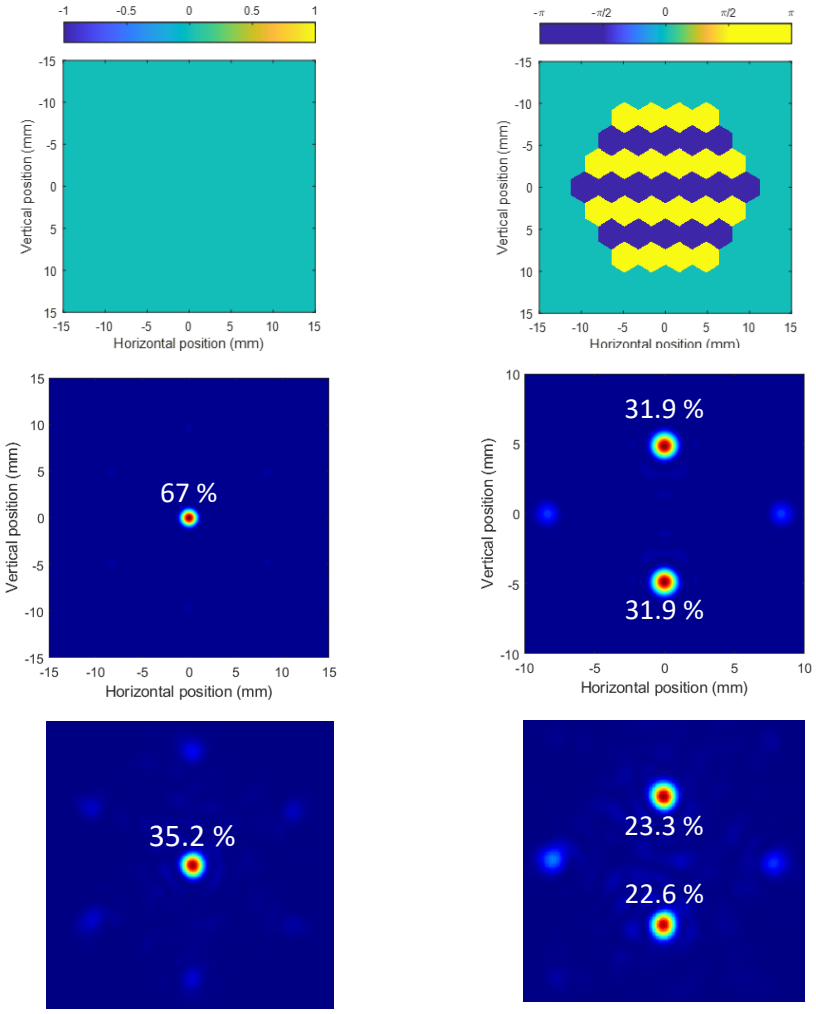

Fig. 5. Left/Right: In-phase/out-of-phase patterns for 37-hexagonal fiber array (top line), simulated and experimental far fields (2nd and 3rd lines). Horizontal and vertical scales are identical for simulated and experimental far fields.

a small energy mismatch between the two lobes. The most significant result here is that dual-beam generated by the out-of-phase pattern contains ~74% of total energy compared to 53% for the main beam obtained with the in-phase pattern, representing thereby 21% improvement for the CBC efficiency.

The main difference from the in-phase pattern is that sidelobes contain much lower energy as they are shifted further away from the center and their intensity drop-down rapidly (Fig. 4 - bottom line). Consequently, the two main lobes carry most of the input energy and could be re-combined through a simple filled aperture setup with high efficiency. This concept is even more interesting in case of lower fill factor where the energy in the sidelobes is important.

Configuration 2: This second configuration consists in a 2D hexagonal array composed of 37 fiber amplifiers (P37), where the phase differences are π between the neighboring fiber-lines.

As shown both by simulation and experimental results (Fig. 5), such phase pattern allows intensity to be steered towards 4 beams. Thus, the far filed is composed of two symmetric

Optics EXPRESS

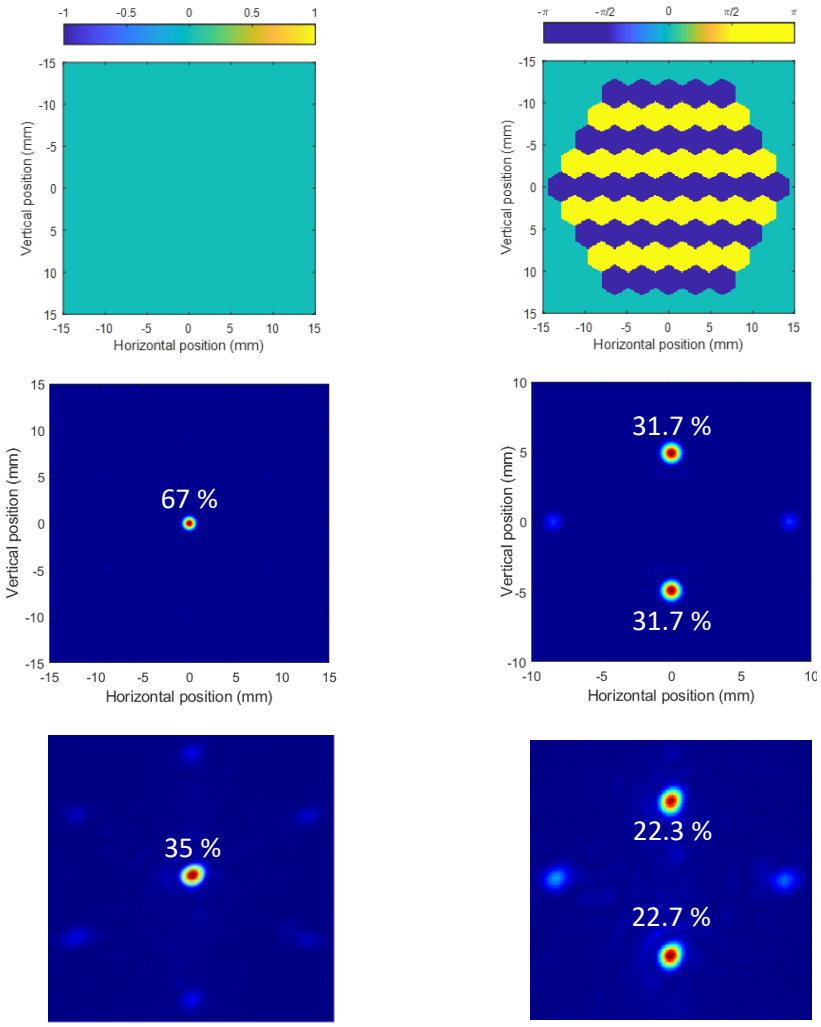

Fig. 6. Left/Right: In-phase/out-of-phase patterns for 61-hexagonal fiber array (top line), simulated and experimental far fields (2nd and 3rd lines). Horizontal and vertical scales are identical for simulated and experimental far fields.

high intensity lobes (Y-axis) and two symmetric low intensity lobes (X-axis). Combining the two powerful beams, leads to an efficiency of 64%, which is not offering an improvement when comparing to the 67% in-phase case (with one main beam), except from a beam shaping interest perspective. However, in view of the experimental results, the efficiencies obtained for the in-phase and the out-of-phase are respectively 35% to ~ 46%, representing thereby 11% improvement for the CBC efficiency.

Configuration 3: This third configuration consists in a 2D hexagonal array composed of 61 fiber amplifiers (P61), where the phase differences are π between the neighboring fiber-lines (Fig. 6).

Compared to configuration 2, 24 more fibers are added to the 2D fiber array. Like in configuration 2, the out-of-phase far field is composed of two symmetric high intensity lobes and two low intensity lobes. Combining the two powerful beams, leads to a simulated potential efficiency of 63%, not so far from the 67% in-phase case (with one main beam). However, the

Optics EXPRESS

experimental results show that the efficiencies obtained for the in-phase and the out-of-phase are respectively 35% to ~ 45%, representing here again 10% improvement for the CBC efficiency.

4. Discussion and conclusion

In this work, the out-of-phase pattern is applied on a full CBC femtosecond laser tiled architecture. For all the studied configurations, the experimental far fields are in excellent agreement with simulations, demonstrating that the out-of-phase concept is suitable for the combination of a large number of fiber amplifiers with broadband ultrashort pulses.

Simulation results for configurations 2 (P37) and 3 (P61) employing an out-of-phase pattern, show that the total CBC efficiency (only taking into account the two high energy main lobes) is not higher when compared to the in-phase pattern (with a single central main lobe). However, the experimental effective CBC efficiencies (with ± 1% uncertainty) are shown to be improved (by 10 to 20%) both for the 1D and 2D fiber array configurations. The out-of-phase pattern allows a "null-field" intensity at lenslets' edges, which reduces energy wastage due to scattering and clipping [13,15]. We believe that a part of the efficiency gain comes from this statement.

Several other effects contribute to CBC efficiency degradation: the main ones being correlated phase errors between the 61 beams [17,18] and misalignments in the 2D hexagonal fiber array. In view of the experimental results, the out-of-phase pattern seems to be more robust to phase errors and beam-to-beam in-homogeneities, resulting in an improved focused intensity far field profile. This assumption may explain why in configurations 2 and 3, the two lobes contain much energy.

The most impressive result concerns configuration 1 (P9 - 1D array) with the out-of-phase pattern. The energy wasted in sidelobes when the in-phase pattern is applied, is re-steered to form two powerful main lobes when the out-of-phase is employed. The out-of-phase concept is even more interesting in case of square fiber array with low fill factor (Fig. 3), where the energy is steered to form 4 main lobes.

Applying a phase difference of π between neighboring fibers or neighboring fiber-lines offers high agility for far field energy distribution control. The main difference with the in-phase pattern is that undesired sidelobes contain much lower energy being shifted further away from the center of the envelope in the far field. It could then be envisioned to combine these generated main beams with a filled aperture approach as a second CBC step, alleviating thus the "unity filling factor" constraint, usually recommended for tiled CBC systems. A favorable approach would be to rely on a set of adequately designed transmissive grating [4]. All in all, differently from the in-phase pattern, when the CBC efficiency is only related to the main lobe energy, with the out-of-phase pattern, the CBC efficiency considers all the main lobes.

Finally, fast beam adjustability offers an extra degree of freedom for various applications requesting polarized double beam (trapping particles,. . .), dynamic energy or power distribution control (beam steering, material processing,. . .) [19,20]. Performing iterative computing approaches like the Gerchberg-Saxton (GS) algorithm [21], deep learning [22] and neural network [23] allows computing the required phase and intensity modulation to be applied on the near field to produce a predefined target far field distribution. This work paves the way for deeper exploration of phase patterns as a tool to further improve the efficiency achievable with tiled-aperture/filled-aperture setups and far field shaping on demand. Foreseen implementation on our experimental setup of individual polarization adjustment could offers more versatility for a fully control of beam shaping and energy distribution. The approaches under investigation for individual control of the polarization of the 61 beams are based on the development of individual rotation actuators. We consider acting directly on the fiber ferules orientation or implementing an array of small aperture half-wave plates after the microlens array. In both cases the difficulty lies in the miniaturization of the actuators with a mm scale pitch.

Funding. Centre National d'Etudes Spatiales (1); Agence de l'innovation de Défense (2).

Optics EXPRESS

Disclosures. The authors declare no conflicts of interest.

Data availability. Date underlying the results presented in this paper are not publicly available at this time but may be obtained from the authors upon reasonable request.

References

1. A. Brignon, (ed.) Coherent Laser Beam Combining, Wiley-VCH, (2013).
2. G. Mourou, B. Brocklesby, T. Tajima, and J. Limpert, "The future is fibre accelerators," Nat. Photonics **7**(4), 258–261 (2013).
3. M. Müller, C. Aleshire, A. Klenke, E. Haddad, F. Légaré, A. Tünnermann, and J. Limpert, "10.4 kW coherently combined ultrafast fiber laser," Opt. Lett. **45**(11), 3083–3086 (2020).
4. T. Zhou, Q. Du, T. Sano, R. Wilcox, and W. Leemans, "Two-dimensional combination of eight ultrashort pulsed beams using a diffractive optic pair," Opt. Lett. **43**(14), 3269–3272 (2018).
5. I. Fsaifes, L. Daniault, S. Bellanger, M. Veinhard, J. Bourderionnet, C. Larat, E. Lallier, E. Durand, A. Brignon, and J.-C. Chanteloup, "Coherent beam combining of 61 femtosecond fiber amplifiers," Opt. Express **28**(14), 20152–20161 (2020).
6. J. Le Dortz, "Mise en phase active de fibres laser en régime femtoseconde par méthode interférométrique," PhD thesis. Université Paris-Saclay, Sept. 2018.
7. J. K. Jabczynski and P. Gontar, "Analysis of the caustics of partially coherently combined truncated Gaussian beams," Appl. Opt. **59**(11), 3340–3346 (2020).
8. D. Zhi, Z. Zhang, Y. Ma, X. Wang, Z. Chen, W. Wu, P. Zhou, and L. Si, "Realization of large energy proportion in the central lobe by coherent beam combination based on conformal projection system," Sci Rep **7**(1), 2199 (2017).
9. G. Forbes, "Shape specification for axially symmetric optical surfaces," Opt. Express **15**(8), 5218–5226 (2007).
10. H. Wang, B. He, Y. Yang, J. Zhou, X. Zhang, Y. Liang, Z. Sun, Y. Lin Song, Y. Wang, and Z. Zhang, "Beam quality improvement of coherent beam combining by gradient power distribution hexagonal tiled-aperture large laser array," Opt. Eng. **58**(6), 1 2019.
11. J. Liao, W. Li, Y. Gao, Y. Tan, Y. Sun, Z. Wang, and J. Lan, "Beam-quality improvement with a bio-inspired sunflower array for coherent beam combining," Appl. Opt. **60**(31), 9713–9720 (2021).
12. B. Liu, Y. Liu, and Y. Braiman, "Coherent beam combining of high power broad-area laser diode array with a closed-V-shape external Talbot cavity," Opt. Express **18**(7), 7361–7368 (2010).
13. R. Huang, B. Chann, L. Missaggia, S. Augst, M. Connors, G. Turner, A. Sanchez-Rubio, J. Donnelly, J. Hostetler, C. Miester, and F. Dorsch, "Coherent combination of slab-coupled optical waveguide lasers," Proc. SPIE 7230, Novel In-Plane Semiconductor Lasers VIII 72301G, 2009.
14. I. Hassiaoui, N. Michel, G. Bourdet, R. Mc Bride, M. Lecomte, O. Parillaud, M. Calligaro, M. Krakowski, and J.-P. Huignard, "Very compact external cavity diffraction-coupled tapered laser diodes," Appl. Opt. **47**(6), 746–750 (2008).
15. A. Andrianov, N. Kalinin, E. Anashkina, and G. Leuchs, "Highly efficient coherent beam combining of tiled aperture arrays using out-of-phase pattern," Opt. Lett. **45**(17), 4774–4777 (2020).
16. M. Veinhard, S. Bellanger, L. Daniault, I. Fsaifes, J. Bourderionnet, C. Larat, E. Lallier, A. Brignon, and J.-C. Chanteloup, "Orbital angular momentum beams generation from 61 channels coherent beam combining femtosecond digital laser," Opt. Lett. **46**(1), 25–28 (2021).
17. C. D. Nabors, "Effects of phase errors on coherent emitter arrays," Appl. Opt. **33**(12), 2284–2289 (1994).
18. B. Rouzé, I. Fsaifes, S. Bellanger, M. Veinhard, T. Rousseaux, J. Primot, J.-C. Chanteloup, and C. Bellanger, "Phase noise measurements and diagnoses of a large array of fiber lasers by PISTIL interferometry," Appl. Opt. **61**(27), 7846–7851 (2022).
19. A. Nissenbaum, N. Armon, and E. Shekel, "Dynamic beam lasers based on coherent beam combining," Proc. SPIE 11981, Fiber Lasers XIX: Technology and Systems 119810B, 2022.
20. M. Prossotowicz, D. Flamm, A. Heimes, F. Jansen, H.-J. Otto, A. Budnicki, A. Killi, and U. Morgner, "Dynamic focus shaping with mixed-aperture coherent beam combining," Opt. Lett. **46**(7), 1660–1663 (2021).
21. R. Gerchberg, "A practical algorithm for the determination of phase from image and diffraction plane pictures," Optik **35**, 237–246 (1972).
22. B. Mills, J. A. Grant-Jacob, M. Praeger, R. W. Eason, J. Nilsson, and M. N. Zervas, "Single step phase optimisation for coherent beam combination using deep learning," Sci Rep **12**(1), 5188 (2022).
23. M. Shpakovych, G. Maulion, A. Boju, P. Armand, A. Barthélémy, A. Desfarges-Berthelemot, and V. Kermene, "On-Demand Phase Control of a 7-Fiber Amplifiers Array with Neural Network and Quasi-Reinforcement Learning," Photonics **9**(4), 243 (2022).